Computed Fractional Flow Reserve (FFT$_{CT}$) Derived from Coronary CT Angiography

Christopher K. Zarins · Charles A. Taylor · James K. Min

Abstract Recent advances in image-based modeling and computational fluid dynamics permit the calculation of coronary artery pressure and flow from typically acquired coronary computed tomography (CT) scans. Computed fractional flow reserve is the ratio of mean coronary artery pressure divided by mean aortic pressure under conditions of simulated maximal coronary hyperemia, thus providing a noninvasive estimate of fractional flow reserve (FFR$_{CT}$) at every point in the coronary tree. Prospective multicenter clinical trials have shown that computed FFR$_{CT}$ improves diagnostic accuracy and discrimination compared to CT stenosis alone for the diagnosis of hemodynamically significant coronary artery disease (CAD), when compared to invasive FFR as the reference gold standard. This promising new technology provides a combined anatomic and physiologic assessment of CAD in a single noninvasive test that can help select patients for invasive angiography and revascularization or best medical therapy. Further evaluation of the clinical effectiveness and economic implications of noninvasive FFR$_{CT}$ are now being explored.

Associate Editor Angela Taylor oversaw the review of this article.

C. K. Zarins (✉) · C. A. Taylor
HeartFlow, Inc., Redwood City, CA, USA
e-mail: zarins@heartflow.com

J. K. Min
Weill Cornell Medical College and New York Presbyterian Hospital, New York, NY, USA

C. K. Zarins · C. A. Taylor
Stanford University, Stanford, CA, USA

Abbreviations

CAD	Coronary artery disease
CCTA	Coronary computed tomographic angiography
ICA	Invasive coronary angiography
CT	Computed tomography
FFR	Fractional flow reserve
FFR$_{CT}$	FFR derived from coronary computed tomography
PCI	Percutaneous coronary intervention
AUC	Area under the receiver operating characteristic curve

Introduction

Invasive coronary angiography (ICA) has served as the cornerstone for the diagnosis of patients with known or suspected coronary artery disease (CAD) and provides a roadmap for interventional and surgical treatment. Decisions regarding coronary revascularization are typically made on an ad hoc basis from visual estimates of the severity of coronary artery luminal narrowing [1]. However, it is well known that coronary angiography has limited value in determining the hemodynamic, or physiologic, significance of coronary lesions, particularly for moderate coronary stenosis [4]. This determination prior to coronary revascularization has been demonstrated as the most important factor to influence clinical outcome in patients with CAD [2, 3]. Patients with ischemia-causing stenoses benefit from revascularization [4, 5] whereas patients with hemodynamically insignificant stenoses require no intervention and experience favorable outcomes on medical therapy alone, with myocardial infarction and mortality rates of <1 % per year [6, 7]. Thus, determination of the hemodynamic significance of coronary lesions is of paramount importance in guiding treatment strategy, and this can be readily accomplished during ICA by measurement of fractional flow reserve (FFR) [8]. Despite remarkable advances in noninvasive cardiac imaging

capabilities, no currently available noninvasive imaging test can reliably diagnose the presence or absence of ischemia-causing stenoses on a lesion-specific basis. The recent introduction of a novel computational method has enabled the calculation of fractional flow reserve (FFR_{CT}) from cardiac computed tomography (CT) imaging data without the need for additional imaging, medication, or modification of CT acquisition protocols [9] [10]. This manuscript will review the rationale of FFR and the scientific basis for noninvasive computational FFR and discuss its clinical application.

Invasive FFR Measurement

Fractional flow reserve measurement is based on the relationship between coronary artery pressure and blood flow. Although this relationship is quite variable at rest, during maximal hyperemia, there is a linear relationship between coronary pressure and flow because peripheral resistance is minimal and therefore constant [11]. FFR is thus defined as the ratio of maximal achievable blood flow through a stenotic artery to maximal flow in the hypothetical case that the artery is normal and is determined by the ratio of pressures across the stenosis during maximal coronary hyperemia [12, 13]. FFR is measured during cardiac catheterization using a guide wire with a pressure-sensing transducer that is placed across the stenotic lesion. After induction of maximal hyperemia using a vasodilating agent such as intravenous or intra-arterial adenosine, the pressure gradient across the lesion is recorded, and FFR is calculated as the mean distal coronary pressure divided by mean aortic pressure. FFR takes into account the contribution of collaterals and provides a threshold of cutoff values for discriminating lesions that do vs. do not cause ischemia [8]. Coronary stenoses with FFR <0.75 are almost always functionally significant whereas lesions with FFR >0.80 are rarely associated with inducible ischemia [13]. Prospective, multicenter, randomized clinical trials have shown that FFR-guided revascularization provides a sustained clinical benefit with improved event-free survival and reduced health-care expenditures compared with the traditional strategy of angiographic stenosis guidance [6, 14, 15]. FFR is now considered to be the standard of care for guiding percutaneous coronary revascularization with class IA European Society of Cardiology and class IIA American Heart Association practice guideline recommendations [16, 17]. Nonetheless, despite unequivocal evidence supporting the use of FFR to guide clinical decision making, adoption into daily clinical practice has been limited, and FFR is currently used in less than 10 % of coronary revascularization procedures in the USA [18]. This may be due in part to the invasive nature of the procedure, the need for pharmacologic vasodilation, and risks related to instrumentation

of the coronary arteries, each of which underscores the need for a noninvasive method to determine the functional significance of individual coronary lesions.

Noninvasive Evaluation of CAD

Noninvasive evaluation of coronary artery disease can be readily performed using multidetector row CT scanners which provide high-resolution anatomic imaging of the coronary arteries and obstructive atherosclerotic plaques [19]. A number of prospective, multicenter studies have demonstrated high diagnostic performance for the identification and exclusion of anatomically obstructive coronary artery disease compared to ICA [20–22]. However, CT cannot determine the hemodynamic significance of coronary lesions and frequently overestimates the severity of stenosis. Even among high-grade stenoses identified by CT and confirmed by angiography, less than half are ischemia causing when compared to FFR [23, 24]. This unreliable relationship between stenosis severity and functional significance has raised concerns that the use of coronary computed tomographic angiography (CCTA) may precipitate unnecessary invasive angiography and unneeded revascularization procedures [25]. Revascularization of nonischemic lesions provides no clinical benefit in terms of improvement of blood flow but nonetheless exposes the patient to the risks of the procedure. Recent randomized trials have shown no survival benefit in patients undergoing angiographically guided coronary revascularization compared to medical treatment alone [26, 27] and have highlighted the need for physiologic testing prior to coronary revascularization.

A number of noninvasive imaging studies provide functional assessment of CAD by identifying regional differences in coronary flow reserve or wall motion abnormalities. While these serve as useful surrogates for ischemia, they do not directly visualize coronary stenoses or assess the hemodynamic significance of individual coronary lesions. Furthermore, noninvasive stress testing misclassifies a significant number of patients as low risk and has significant false-positive and false-negative rates resulting in many patients having no evidence of obstructive CAD when studied by ICA [28, 29]. Accordingly, some have advocated for hybrid imaging with physiologic and anatomic evaluation of CAD by stress testing and CT [30]. However, this approach requires two tests and is associated with higher costs and a greater radiation burden for the patient. A long-standing goal of noninvasive imaging of CAD has been to provide physicians with a single test that identifies high-grade stenosis and determines the functional significance of identified lesions. This has been described as the elusive "holy grail" of noninvasive CAD imaging [31]. The addition of computational FFR analysis to the anatomic imaging capabilities of CT

710

J. of Cardiovasc. Trans. Res. (2013) 6:708–714

provides such a combined anatomic–physiologic assessment of CAD from a single imaging test.

Computational Analysis of Blood Flow Based on CT

While computational analysis of airflow has been a mainstay of aircraft and automotive design for more than 50 years, computational fluid dynamics has only recently been applied to the human circulatory system for evaluation of blood flow. Initial applications involved the study of flow characteristics in the carotid bifurcation [32], followed by image-based modeling of pulsatile blood flow in the abdominal aorta and aortic aneurysms [33]. The key element for the realistic modeling of human blood flow is precise 3D anatomic imaging of the vasculature that can now be readily provided by contrast-enhanced computed tomography. In addition, numerical methods which incorporate physiologic boundary conditions of the circulation are needed in order to construct patient-specific computational blood flow [34]. The introduction of 64-detector row CT scanners provided accurate anatomic images of the moving heart that made it possible to build patient-specific 3D computational models of the coronary vasculature. The calculation of coronary blood flow required development of specific methods appropriate to the unique physiologic boundary conditions of the coronary circulation [35, 36]. This allowed the computation of coronary velocity and pressure under a variety of conditions including rest, exercise, and physiologically induced coronary hyperemia flow by modification of the boundary conditions. Thus, fractional flow reserve could be calculated as the ratio of distal coronary pressure divided by the proximal aortic pressure under simulated conditions of maximal hyperemia, much the same as when measured FFR is determined during invasive coronary angiography [10].

Scientific Basis for Computation of FFR

The scientific basis for noninvasive quantification of FFR from coronary CT has been described in detail by Taylor et al. [10]. It is based on three underlying principles for the generation of physiologic models of coronary blood flow. The first principle is that baseline coronary blood flow is proportional to myocardial oxygen demand at rest. This enables calculation of total resting coronary blood flow relative to patient-specific myocardial mass that can be quantified on the CT scan. The second principle is that the resistance of the microcirculatory vascular bed at rest is inversely, but not linearly, proportional to the size of the feeding vessel, as has been demonstrated in prior morphometry, shear stress autoregulation, and compensatory remodeling research [37–39]. In other words, healthy and diseased

blood vessels are properly sized and adapt to the amount of flow they carry. The third principle states that the coronary microcirculation has a predictable vasodilatory response to adenosine [40]. When the myocardium lacks oxygen, ATP breaks down with a resulting release of endogenous adenosine. Exogenous administration of adenosine elicits an increase in coronary blood flow with a maximum hyperemic response by producing complete relaxation of smooth muscle cells lining the resistance arterioles. This predictable response allows simulation of maximum hyperemia in the computational model. Thus, FFR is computed by applying a dynamic physiologic model of coronary flow to patient-specific coronary anatomy as revealed by the coronary CT scan. This coronary CT scan can be performed in the usual manner, using standard acquisition protocols, with no need for additional imaging or radiation exposure and no need for adenosine administration.

Computation of FFR from Coronary CT

Computation of FFR from coronary CT involves three basic elements: (1) constructing an accurate patient-specific anatomic model of the epicardial coronary arteries, (2) specifying inflow and outflow boundary conditions reflecting patient-specific coronary physiology during maximal hyperemia, and (3) performing a numerical solution of the laws of physics governing fluid dynamics. This combination of anatomy, physiology, and computational fluid dynamics enables the calculation of coronary artery blood flow and pressure under conditions of maximum hyperemia [10].

Computation of coronary flow and pressure is based on the governing equations of fluid dynamics, which are founded in the relationship between conservation of mass and momentum balance. These equations are known as the "Navier Stokes equations" and have existed in their current form for more than 150 years. The equations are solved for coronary flow and pressure as a function of three spatial coordinates and time. The physical properties of blood (fluid density and fluid viscosity) are assumed, and blood is treated as an incompressible Newtonian fluid with a constant viscosity in the coronary arteries. Since the governing equations of blood flow are nonlinear partial differential equations which can only be solved analytically under highly idealized circumstances, solutions for realistic patient-specific models of the coronary tree require a numerical approximation for velocity and pressure at a finite, but very large, number of points [41]. This requires the computation of millions of nonlinear equations simultaneously and repeating this process for thousands of time intervals in a single cardiac cycle. In addition, it is necessary to define the boundary conditions that interface the modeled domain to the remainder of the circulation; this represents the biggest challenge in blood

flow modeling. Realistic modeling of coronary flow requires coupling of lumped parameter models of the heart, systemic circulation, and coronary circulation to a patient-specific model of the root of the aorta and epicardial coronary arteries extracted from CCTA data [10]. These lumped parameter models combine peripheral resistance, blood vessel compliance, and other factors into distinct elements dependent on the specific parameters of each circulatory bed. Importantly, neither pressure nor flow rate is directly specified at the boundaries of the 3D model, but instead arises naturally from the interaction between the 3D model and the lumped parameter models representing cardiac output, aortic pressure, and microcirculatory resistance [10]. As a final step, the boundary condition of maximum coronary hyperemia is modeled by simulating the effect that adenosine has on reducing the peripheral resistance of the downstream microcirculatory coronary bed.

Clinical Validation of Computed FFR

Clinical validation of computed FFR is based on a direct comparison to measured FFR during invasive coronary angiography. The diagnostic accuracy of noninvasive FFR_{CT} to identify or exclude functionally significant coronary stenoses has been evaluated in two prospective, multicenter studies using measured FFR as the reference standard. The first of these—the Diagnosis of Ischemia-Causing Stenosis Obtained via Non-invasive Fractional Flow Reserve (DISCOVER-FLOW) study—evaluated the diagnostic performance of FFR_{CT} compared to CT stenosis severity using measured FFR as the reference standard [9]. The study was conducted at four clinical sites in the USA, Europe, and Asia and included 103 stable patients with known or suspected CAD who underwent CCTA, ICA, measurement of FFR, and computation of FFR_{CT}. Lesion-specific ischemia was defined as measured FFR ≤0.8 in accord with prior invasive FFR trials [4]. Obstructive coronary artery disease was defined as stenosis ≥50 % on CCTA as measured by a CT core laboratory. Diagnostic performance of FFR_{CT} was superior to CT, and the primary endpoint was met with a per-vessel diagnostic accuracy for FFR_{CT} of 84 % (95 % CI 78–90 %) compared to 59 % (95 % CI 50–66 %) for CT alone. This 42 % improvement was primarily due to a 70 % reduction of false positives. Among the 159 vessels studied, the sensitivity, specificity, positive predictive value, negative predictive value, and accuracy of FFR_{CT} were 88, 82, 74, 92, and 84 %, respectively. While CT alone had a high sensitivity (91 %) and negative predictive value (89 %), CCTA suffered from a low specificity (40 %) and low positive predictive value (47 %). FFR_{CT} increased the specificity of identifying hemodynamically significant stenoses to 82 % compared to 40 % for CT alone. Further, the ability of FFR_{CT} to discriminate

ischemia-producing stenoses from those lesions not producing ischemia was significantly improved with an increase in the area under the curve (AUC) of the receiver operating characteristics curve (0.90) compared to CCTA (0.75) [difference 0.15, $p<0.001$] [9].

Subsequently, the Determination of Fractional Flow Reserve by Anatomic Computed Tomographic Angiography (DeFACTO) study—an international multicenter study involving 252 stable patients with suspected or known CAD from 17 centers in five countries—was performed. The diagnostic accuracy of FFR_{CT} plus CT for the diagnosis of hemodynamically significant coronary stenosis was assessed using measured FFR as the reference standard [42]. Among the 252 patients, 137 (54 %) had evidence of coronary ischemia with a measured FFR of ≤0.80. FFR_{CT} demonstrated improved accuracy for the diagnosis of ischemia compared to CT alone—73 % (95 % CI 67–78 %) for FFR_{CT} vs. 64 % (95 % CI 58–70 %) for CT—but did not satisfy the prespecified primary endpoint of diagnostic accuracy of greater than 70 % of the lower-bound one-sided 95 % confidence interval. When FFR_{CT} was compared to CT for the ability to discriminate patients with and without ischemia, FFR_{CT} demonstrated superior discrimination with the AUC in the ROC analysis of 0.81 compared to 0.68 for CT alone (difference 0.13, $p<0.001$). Similarly, FFR_{CT} demonstrated superior discrimination of ischemia on a per-vessel basis (AUC for FFR_{CT} 0.81 vs. 0.75 for CT, $p<0.001$) [43].

Case examples:

Two case examples from the DeFACTO study demonstrate the benefit of FFR_{CT} in differentiating functional significance in vessels with anatomically obstructive stenoses [43].

Case 1: CCTA demonstrates significant CAD with >50 % lumen stenosis in the left anterior descending (LAD) artery. This is confirmed by quantitative angiography with a stenosis of 57 %. The computational model based on the CT data demonstrates a hemodynamically significant lesion with FFR_{CT} in the distal LAD of 0.62. The measured FFR during invasive angiography is 0.65.
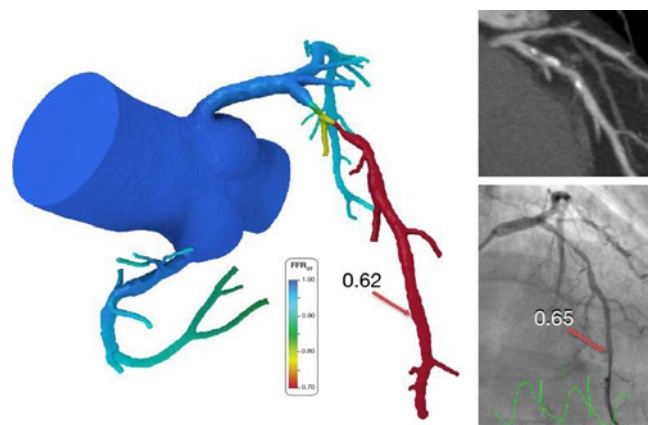
Case 2:   CCTA demonstrates >50 % stenosis in the mid
right coronary artery (RCA). The angiogram
demonstrates a significant lesion in the RCA
which measured 62 % stenosis by quantitative
coronary angiography. Computed FFR_{CT} is 0.87
indicating a nonfunctionally significant stenosis.
This was confirmed by a measured FFR of
0.86. Such nonfunctionally significant lesions
have a favorable outlook when treated medically
[6, 7].
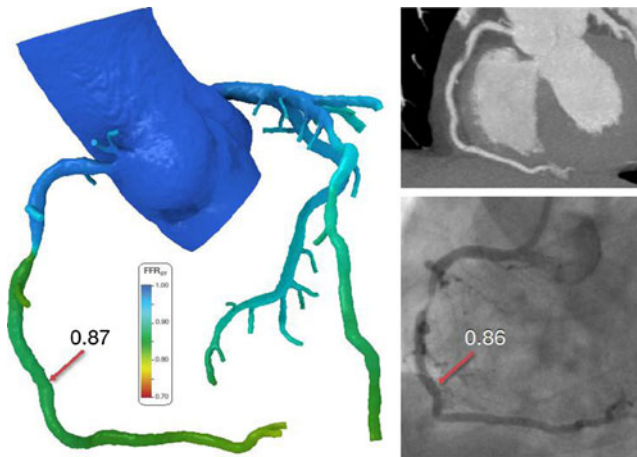
Intermediate Stenosis

Intermediate-severity coronary stenoses often cause ische-
mia, but differentiating between hemodynamically signifi-
cant and nonfunctional intermediate lesions is challenging,
both for noninvasive imaging as well as for invasive angi-
ography. Among 103 patients in the DISCOVER-FLOW
study, 60 patients (58 %) had intermediate stenosis of 40–
69 % by quantitative coronary angiography. Computation of
FFR_{CT} improved the accuracy of identifying functionally
significant lesions to 86 % compared to 56 % for CT alone.
This was primarily due to a threefold improvement in spec-
ificity (83 % compared to only 26 % for CT alone). There
was a marked improvement in the ability to discriminate
ischemia-causing stenosis with an AUC in the receiver op-
erating characteristics curve of 0.95 for FFR_{CT} ($p<0.0001$
compared to CT alone) [43].

Potential Limitations

A number of potential limitations exist that may influence the
diagnostic performance of FFR_{CT}, most notably impaired
coronary CT image quality. Significant CT imaging artifacts
include misalignment, motion, beam hardening from coronary

calcification, and increased image noise. These issues can be
minimized by close adherence to CCTA image acquisition
guidelines [44], in particular by use of beta blockers to reduce
heart rate and heart rate variability as well as administration of
sublingual nitrates to dilate the coronary arteries. In the clin-
ical studies of FFR_{CT}, CT image quality was evaluated by
independent core laboratories, and all patients judged to have
evaluable images were included for FFR_{CT} analysis. In the
DeFACTO study, 11 % of patients were judged by the core
laboratory to have nonevaluable CT images and were excluded
from the study. Given the dependence of FFR_{CT} on accurate
coronary segmentation for proper image-based modeling,
excellent image quality should remain a primary goal of
cardiac CT imaging.

In addition, diagnostic performance of FFR_{CT} compared
to measured FFR may be affected by patient-specific differ-
ences in responsiveness of the microcirculation to vasodila-
tors and physiologic conditions which may affect assumed
parameters such as fluid density and viscosity. Viscosity is
assumed from hematocrit/hemoglobin concentration and,
when in the normal range, has minimal influence on FFR_{CT}.
However, under conditions of severe anemia, reduced vis-
cosity may impact calculation of FFR_{CT}. The magnitude of
such an impact is not yet known.

To date, evaluation of FFR_{CT} has been limited to a
population of stable patients with known or suspected
coronary artery disease who were undergoing coronary
angiography. Patients with prior CABG or PCI with
suspected in-stent restenosis were excluded from the
studies as were patients with acute coronary syndrome
or within 30 days of myocardial infarction [43]. Thus,
generalizability to broader populations of patients with
CAD is unknown. Finally, outcomes data are not yet
available, and it is unknown whether revascularization
of the ischemic lesions identified by FFR_{CT} will achieve
reduction in ischemia from revascularization.

Conclusion

Noninvasive assessment of the functional significance of
coronary stenoses is now possible using computationally
derived fractional flow reserve from anatomic coronary CT
data. This promising new technology provides a combined
anatomic–functional assessment of coronary artery disease
using a single noninvasive test with the goal of helping
physicians appropriately select patients for medical therapy
or invasive angiography to improve clinical outcomes while
reducing health-care costs.

J. of Cardiovasc. Trans. Res. (2013) 6:708–714

713

References

1. Lucas, F. L., Siewers, A. E., Malenka, D. J., & Wennberg, D. E. (2008). Diagnostic-therapeutic cascade revisited: coronary angiography, coronary artery bypass graft surgery, and percutaneous coronary intervention in the modern era. *Circulation, 118*, 2797–2802.

2. Shaw, L. J., & Iskandrian, A. E. (2004). Prognostic value of gated myocardial perfusion SPECT. *Journal of Nuclear Cardiology, 11*, 171–185.

3. Metz, L. D., Beattie, M., Hom, R., Redberg, R. F., Grady, D., & Fleischmann, K. E. (2007). The prognostic value of normal exercise myocardial perfusion imaging and exercise echocardiography: a meta-analysis. *Journal of the American College of Cardiology, 49*, 227–237.

4. Tonino, P. A., De Bruyne, B., Pijls, N. H., Siebert, U., Ikeno, F., van 't Veer, M., Klauss, V., Manoharan, G., Engstrom, T., Oldroyd, K. G., Ver Lee, P. N., MacCarthy, P. A., & Fearon, W. F. (2009). Fractional flow reserve versus angiography for guiding percutaneous coronary intervention. *New England Journal of Medicine, 360*, 213–224.

5. Shaw, L. J., Heller, G. V., Casperson, P., Miranda-Peats, R., Slomka, P., Friedman, J., Hayes, S. W., Schwartz, R., Weintraub, W. S., Maron, D. J., Dada, M., King, S., Teo, K., Hartigan, P., Boden, W. E., O'Rourke, R. A., & Berman, D. S. (2006). Gated myocardial perfusion single photon emission computed tomography in the clinical outcomes utilizing revascularization and aggressive drug evaluation (COURAGE) trial, veterans administration cooperative study no. 424. *Journal of Nuclear Cardiology, 13*, 685–698.

6. Pijls, N. H., Fearon, W. F., Tonino, P. A., Siebert, U., Ikeno, F., Bornschein, B., van't Veer, M., Klauss, V., Manoharan, G., Engstrom, T., Oldroyd, K. G., Ver Lee, P. N., MacCarthy, P. A., & De Bruyne, B. (2010). Fractional flow reserve versus angiography for guiding percutaneous coronary intervention in patients with multivessel coronary artery disease: 2-year follow-up of the FAME (Fractional Flow Reserve Versus Angiography for Multivessel Evaluation) study. *Journal of the American College of Cardiology, 56*, 177–184.

7. Pijls, N. H., van Schaardenburgh, P., Manoharan, G., Boersma, E., Bech, J. W., van't Veer, M., Bar, F., Hoorntje, J., Koolen, J., Wijns, W., & de Bruyne, B. (2007). Percutaneous coronary intervention of functionally nonsignificant stenosis: 5-year follow-up of the DEFER study. *Journal of the American College of Cardiology, 49*, 2105–2111.

8. Pijls, N. H., & Sels, J. W. (2012). Functional measurement of coronary stenosis. *Journal of the American College of Cardiology, 59*, 1045–1057.

9. Koo, B. K., Erglis, A., Doh, J. H., Daniels, D. V., Jegere, S., Kim, H. S., Dunning, A., DeFrance, T., Lansky, A., Leipsic, J., & Min, J. K. (2011). Diagnosis of ischemia-causing coronary stenoses by noninvasive fractional flow reserve computed from coronary computed tomographic angiograms. Results from the prospective multicenter DISCOVER-FLOW (Diagnosis of Ischemia-Causing Stenoses Obtained Via Noninvasive Fractional Flow Reserve) study. *Journal of the American College of Cardiology, 58*, 1989–1997.

10. Taylor, C. A., Fonte, T. A., & Min, J. K. (2013). Computational fluid dynamics applied to cardiac computed tomography for noninvasive quantification of fractional flow reserve: scientific basis. *Journal of the American College of Cardiology., 61*, 2233–2241.

11. Pijls, N. H., van Son, J. A., Kirkeeide, R. L., De Bruyne, B., & Gould, K. L. (1993). Experimental basis of determining maximum coronary, myocardial, and collateral blood flow by pressure measurements for assessing functional stenosis severity before and after percutaneous transluminal coronary angioplasty. *Circulation, 87*, 1354–1367.

12. De Bruyne, B., Baudhuin, T., Melin, J. A., Pijls, N. H., Sys, S. U., Bol, A., Paulus, W. J., Heyndrickx, G. R., & Wijns, W. (1994). Coronary flow reserve calculated from pressure measurements in humans. Validation with positron emission tomography. *Circulation, 89*, 1013–1022.

13. Pijls, N. H., Van Gelder, B., Van der Voort, P., Peels, K., Bracke, F. A., Bonnier, H. J., & el Gamal, M. I. (1995). Fractional flow reserve. A useful index to evaluate the influence of an epicardial coronary stenosis on myocardial blood flow. *Circulation, 92*, 3183–3193.

14. Fearon, W. F., Bornschein, B., Tonino, P. A., Gothe, R. M., Bruyne, B. D., Pijls, N. H., & Siebert, U. (2010). Economic evaluation of fractional flow reserve-guided percutaneous coronary intervention in patients with multivessel disease. *Circulation, 122*, 2545–2550.

15. De Bruyne, B., Pijls, N. H., Kalesan, B., Barbato, E., Tonino, P. A., Piroth, Z., Jagic, N., Mobius-Winkler, S., Rioufol, G., Witt, N., Kala, P., MacCarthy, P., Engstrom, T., Oldroyd, K. G., Mavromatis, K., Manoharan, G., Verlee, P., Frobert, O., Curzen, N., Johnson, J. B., Juni, P., & Fearon, W. F. (2012). Fractional flow reserve-guided PCI versus medical therapy in stable coronary disease. *The New England Journal of Medicine, 367*, 991–1001.

16. Wijns, W., Kolh, P., Danchin, N., Di Mario, C., Falk, V., Folliguet, T., Garg, S., Huber, K., James, S., Knuuti, J., Lopez-Sendon, J., Marco, J., Menicanti, L., Ostojic, M., Piepoli, M. F., Pirlet, C., Pomar, J. L., Reifart, N., Ribichini, F. L., Schalij, M. J., Sergeant, P., Serruys, P. W., Silber, S., Sousa Uva, M., & Taggart, D. (2010). Guidelines on myocardial revascularization. *European Heart Journal, 31*, 2501–2555.

17. Levine, G. N., Bates, E. R., Blankenship, J. C., Bailey, S. R., Bittl, J. A., Cercek, B., Chambers, C. E., Ellis, S. G., Guyton, R. A., Hollenberg, S. M., Khot, U. N., Lange, R. A., Mauri, L., Mehran, R., Moussa, I. D., Mukherjee, D., Nallamothu, B. K., & Ting, H. H. (2011). ACCF/AHA/SCAI guideline for percutaneous coronary intervention. A report of the American College of Cardiology Foundation/American Heart Association Task Force on Practice Guidelines and the Society for Cardiovascular Angiography and Interventions. *Journal of the American College of Cardiology, 58*, e44–e122.

18. Kleiman, N. S. (2011). Bringing it all together: integration of physiology with anatomy during cardiac catheterization. *Journal of the American College of Cardiology, 58*, 1219–1221.

19. Min, J. K., Shaw, L. J., & Berman, D. S. (2010). The present state of coronary computed tomography angiography a process in evolution. *Journal of the American College of Cardiology, 55*, 957–965.

20. Budoff, M. J., Dowe, D., Jollis, J. G., Gitter, M., Sutherland, J., Halamert, E., Scherer, M., Bellinger, R., Martin, A., Benton, R., Delago, A., & Min, J. K. (2008). Diagnostic performance of 64-multidetector row coronary computed tomographic angiography for evaluation of coronary artery stenosis in individuals without known coronary artery disease: results from the prospective multicenter accuracy (Assessment by Coronary Computed Tomographic Angiography of Individuals Undergoing Invasive Coronary Angiography) trial. *Journal of the American College of Cardiology, 52*, 1724–1732.

21. Miller, J. M., Rochitte, C. E., Dewey, M., Arbab-Zadeh, A., Niinuma, H., Gottlieb, I., Paul, N., Clouse, M. E., Shapiro, E. P., Hoe, J., Lardo, A. C., Bush, D. E., de Roos, A., Cox, C., Brinker, J., & Lima, J. A. (2008). Diagnostic performance of coronary angiography by 64-row CT. *The New England Journal of Medicine, 359*, 2324–2336.

22. Meijboom, W. B., Meijs, M. F., Schuijf, J. D., Cramer, M. J., Mollet, N. R., van Mieghem, C. A., Nieman, K., van Werkhoven, J. M., Pundziute, G., Weustink, A. C., de Vos, A. M., Pugliese, F., Rensing, B., Jukema, J. W., Bax, J. J., Prokop, M., Doevendans, P. A., Hunink, M. G., Krestin, G. P., & de Feyter, P. J. (2008). Diagnostic accuracy of 64-slice computed tomography coronary angiography: a prospective, multicenter, multivendor study. *Journal of the American College of Cardiology, 52*, 2135–2144.

23. Meijboom, W. B., Van Mieghem, C. A., van Pelt, N., Weustink, A., Pugliese, F., Mollet, N. R., Boersma, E., Regar, E., van Geuns, R. J., de Jaegere, P. J., Serruys, P. W., Krestin, G. P., & de Feyter, P. J. (2008). Comprehensive assessment of coronary artery stenoses: computed tomography coronary angiography versus conventional coronary angiography and correlation with fractional flow reserve in patients with stable angina. *Journal of the American College of Cardiology, 52*, 636–643.

24. Schuijf, J. D., & Bax, J. J. (2008). CT angiography: an alternative to nuclear perfusion imaging? *Heart, 94*, 255–257.

25. Nissen, S. E. (2008). Limitations of computed tomography coronary angiography. *Journal of the American College of Cardiology, 52*, 2145–2147.

26. Boden, W. E., O'Rourke, R. A., Teo, K. K., Hartigan, P. M., Maron, D. J., Kostuk, W. J., Knudtson, M., Dada, M., Casperson, P., Harris, C. L., Chaitman, B. R., Shaw, L., Gosselin, G., Nawaz, S., Title, L. M., Gau, G., Blaustein, A. S., Booth, D. C., Bates, E. R., Spertus, J. A., Berman, D. S., Mancini, G. B., & Weintraub, W. S. (2007). Optimal medical therapy with or without PCI for stable coronary disease. *The New England Journal of Medicine, 356*, 1503–1516.

27. Frye, R. L., August, P., Brooks, M. M., Hardison, R. M., Kelsey, S. F., MacGregor, J. M., Orchard, T. J., Chaitman, B. R., Genuth, S. M., Goldberg, S. H., Hlatky, M. A., Jones, T. L., Molitch, M. E., Nesto, R. W., Sako, E. Y., & Sobel, B. E. (2009). A randomized trial of therapies for type 2 diabetes and coronary artery disease. *The New England Journal of Medicine, 360*, 2503–2515.

28. Hendel, R. C., Berman, D. S., Di Carli, M. F., Heidenreich, P. A., Henkin, R. E., Pellikka, P. A., Pohost, G. M., & Williams, K. A. (2009). ACCF/ASNC/ACR/AHA/ASE/SCCT/SCMR/SNM 2009 Appropriate use criteria for cardiac radionuclide imaging: a report of the American College of Cardiology Foundation Appropriate Use Criteria Task Force, the American Society of Nuclear Cardiology, the American College of Radiology, the American Heart Association, the American Society of Echocardiography, the Society of Cardiovascular Computed Tomography, the Society for Cardiovascular Magnetic Resonance, and the Society of Nuclear Medicine. *Journal of the American College of Cardiology, 53*, 2201–2229.

29. Berman, D. S., Kang, X., Slomka, P. J., Gerlach, J., de Yang, L., Hayes, S. W., Friedman, J. D., Thomson, L. E., & Germano, G. (2007). Underestimation of extent of ischemia by gated SPECT myocardial perfusion imaging in patients with left main coronary artery disease. *Journal of Nuclear Cardiology, 14*, 521–528.

30. Gaemperli, O., Bengel, F. M., & Kaufmann, P. A. (2011). Cardiac hybrid imaging. *European Heart Journal., 32*, 2100–2108.

31. Patel, M. R. (2012). Detecting obstructive coronary disease with CT angiography and noninvasive fractional flow reserve. *JAMA, 308*, 1269–1270.

32. Perktold, K., Resch, M., & Peter, R. O. (1991). Three-dimensional numerical analysis of pulsatile flow and wall shear stress in the carotid artery bifurcation. *Journal of Biomechanics, 24*, 409–420.

33. Taylor, C. A., Hughes, T. J. R., & Zarins, C. K. (1996). Computational investigations in vascular disease. *Computers in Physics, 10*, 224–232.

34. Taylor, C. A., & Figueroa, C. A. (2009). Patient-specific modeling of cardiovascular mechanics. *Annual Review of Biomedical Engineering, 11*, 109–134.

35. Kim, H. J., Vignon-Clementel, I. E., Coogan, J. S., Figueroa, C. A., Jansen, K. E., & Taylor, C. A. (2010). Patient-specific modeling of blood flow and pressure in human coronary arteries. *Annals of Biomedical Engineering, 38*, 3195–3209.

36. Kim, H. J., Jansen, K. E., & Taylor, C. A. (2010). Incorporating autoregulatory mechanisms of the cardiovascular system in three-dimensional finite element models of arterial blood flow. *Annals of Biomedical Engineering, 38*, 2314–2330.

37. Glagov, S., Weisenberg, E., Zarins, C. K., Stankunavicius, R., & Kolettis, G. J. (1987). Compensatory enlargement of human atherosclerotic coronary arteries. *The New England Journal of Medicine, 316*, 1371–1375.

38. Zarins, C. K., Zatina, M. A., Giddens, D. P., Ku, D. N., & Glagov, S. (1987). Shear stress regulation of artery lumen diameter in experimental atherogenesis. *Journal of Vascular Surgery, 5*, 413–420.

39. Kamiya, A., & Togawa, T. (1980). Adaptive regulation of wall shear stress to flow change in the canine carotid artery. *American Journal of Physiology, 239*, H14–H21.

40. Wilson, R. F., Wyche, K., Christensen, B. V., Zimmer, S., & Laxson, D. D. (1990). Effects of adenosine on human coronary arterial circulation. *Circulation, 82*, 1595–1606.

41. Taylor, C. A., Hughes, T. J., & Zarins, C. K. (1998). Finite element modeling of three-dimensional pulsatile flow in the abdominal aorta: relevance to atherosclerosis. *Annals of Biomedical Engineering, 26*, 975–987.

42. Min, J. K., Leipsic, J., Pencina, M. J., Berman, D. S., Koo, B. K., van Mieghem, C., Erglis, A., Lin, F. Y., Dunning, A. M., Apruzzese, P., Budoff, M. J., Cole, J. H., Jaffer, F. A., Leon, M. B., Malpeso, J., Mancini, G. B., Park, S. J., Schwartz, R. S., Shaw, L. J., & Mauri, L. (2012). Diagnostic accuracy of fractional flow reserve from anatomic CT angiography. *Journal of the American Medical Association, 308*, 1237–1245.

43. Min, J. K., Koo, B. K., Erglis, A., Doh, J. H., Daniels, D. V., Jegere, S., Kim, H. S., Dunning, A. M., Defrance, T., Lansky, A., & Leipsic, J. (2012). Usefulness of noninvasive fractional flow reserve computed from coronary computed tomographic angiograms for intermediate stenoses confirmed by quantitative coronary angiography. *The American Journal of Cardiology, 110*, 971–976.

44. Nam, C. W., Mangiacapra, F., Entjes, R., Chung, I. S., Sels, J. W., Tonino, P. A., De Bruyne, B., Pijls, N. H., & Fearon, W. F. (2011). Functional syntax score for risk assessment in multivessel coronary artery disease. *Journal of the American College of Cardiology, 58*, 1211–1218.